Max-Planck-Institut
für Mathematik
in den Naturwissenschaften
Leipzig

The critical role of the base curve for the qualitative behavior of shearable rods

by

Stuart S. Antman and Friedemann Schuricht

Preprint no.: 67 2001

The Critical Role of the Base Curve for the Qualitative Behavior of Shearable Rods

Stuart S. Antman
Department of Mathematics
Institute for Physical Science and Technology
and Institute for Systems Research
University of Maryland
College Park, MD 20742-4015, U.S.A.
e-mail: ssa@math.umd.edu
and
Friedemann Schuricht
Max-Planck-Institut for Mathematics in the Sciences
Inselstr. 22 - 26, 04103 Leipzig, Germany
e-mail: schur@mis.mpg.de

Abstract

This paper treats several aspects of the *induced* geometrically exact theory of shearable rods, of central importance for contact problems, for which the regularity of solutions depends crucially on the presence of shearability. (An *induced* theory is one derived from the 3-dimensional theory by the imposition of constraints. Because the role of thickness enters into our theory in an essential way, it is an exact version of what has been called the theory of "moderately thick" rods.) In particular, we study how the theory and constitutive restrictions depend upon the choice of the base curve, and we show how this choice has major qualitative consequences, which are illustrated with several concrete examples.

1 Introduction

The Euler-Bernoulli theory [5] of the elastica describes planar equilibrium states of inextensible, unshearable elastic rods with the bending couple at a section depending linearly on the difference in the curvature at that section between its values at the deformed and natural configurations. Kirchhoff [6] extended this theory to rods that can deform in 3-dimensional space, undergoing flexure and torsion. The Cosserats [4] formulated theories of rods that furthermore could suffer shear and both longitudinal and transverse extension. The version of this theory for the small planar deformation of rods with no transverse extension was developed by Timoshenko [11]. These *refined* theories of rods describe effects of limited importance in some traditional civil engineering applications of the theory of rods (other than buckling), but are of greater importance in more modern applications of structural mechanics (possibly including physiological applications). The role of shearability is central not only for buckling problems [1], but also for contact problems, in which the regularity of the solution depends critically on it [8]. Contact problems form one of the main motivations for our study.

When rod theories are constructed by imposing holonomic constraints on the 3-dimensional theory of elasticity, the Strong Ellipticity Condition directly yields a class of very useful monotonicity conditions on the constitutive functions of the 1-dimensional theory [1]. For certain problems, particularly contact problems, these restrictions fail to prevent certain behavior that may be regarded as surprising [10]. To preclude such behavior it is necessary to impose further constitutive restrictions. As we shall see, such constitutive restrictions for contact problems are not easily related to others useful for other kinds of problems.

In Section 2 we outline our geometrically exact theory for the planar equilibrium states of shearable nonlinearly elastic rods obtained by constraining the deformation and employing the Principle of Virtual Work. The configurations of these rods are determined by a choice of base curve and a family of sections. In Section 3, we treat the interesting and surprisingly rich question of determining when two such theories based on different choices of base curves and sections are equivalent. The transformation formulas we obtain are used in the treatment of examples in Section 5. In Section 4 we discuss constitutive restrictions associated with the curvature of the base curve. These restrictions play a central role in Section 5.

Notation. We employ Gibbs notation for vectors and tensors (the latter used infrequently): Vectors, which are elements of Euclidean 3-space $\mathbb{E}^3$, and vector-valued functions are denoted by lower-case, italic, bold-face symbols. The dot product of (vectors) $\boldsymbol{u}$ and $\boldsymbol{v}$ is denoted by $\boldsymbol{u}\cdot\boldsymbol{v}$. A (second-order) tensor is just a linear transformation from $\mathbb{E}^3$ to itself. The value of tensor $\boldsymbol{A}$ at vector $\boldsymbol{v}$ is denoted $\boldsymbol{A}\cdot\boldsymbol{v}$ (in place of the more usual $\boldsymbol{A}\boldsymbol{v}$) and the product of $\boldsymbol{A}$ and $\boldsymbol{B}$ is denoted $\boldsymbol{A}\cdot\boldsymbol{B}$ (in place of the more usual $\boldsymbol{A}\boldsymbol{B}$). The transpose of $\boldsymbol{A}$ is denoted $\boldsymbol{A}^*$. We write $\boldsymbol{u}\cdot\boldsymbol{A} = \boldsymbol{A}^*\cdot\boldsymbol{u}$. The dyadic product of vectors $\boldsymbol{a}$ and $\boldsymbol{b}$ is the tensor denoted $\boldsymbol{a}\boldsymbol{b}$ (in place of the more usual $\boldsymbol{a}\otimes\boldsymbol{b}$), which is defined by $(\boldsymbol{a}\boldsymbol{b})\cdot\boldsymbol{u} = (\boldsymbol{b}\cdot\boldsymbol{u})\boldsymbol{a}$ for all $\boldsymbol{u}$.

2 Induced Rod Theories

A hierarchy of rod theories can be constructed by describing a slender rod-like body as a union of a family of sections and then imposing holonomic constraints that endow each section with but a finite number of degrees of freedom. (To these constraints may be added nonholonomic constraints like that of incompressibility [2].) If $\boldsymbol{\varphi}(\mathbf{x},t)$ denotes the position at time t of the material point with a triple of curvilinear coordinates $\mathbf{x} = (s,x,y)$, then a holonomic (and scleronomic) constraint restricting the section with coordinate s to n degrees of freedom has the form

$$\boldsymbol{\varphi}(\mathbf{x},t) = \boldsymbol{\pi}(\mathbf{u}(s,t),\mathbf{x}) \tag{2.1}$$

where the set $\mathbf{u}$ of generalized coordinates lies in an n-dimensional space [1, Chap. 14]. To be specific, we limit our attention to planar deformations of rods the configurations of which are determined by a plane curve, the *base* curve, representing the configuration of some convenient material curve, and by the orientations of sections with respect to the base curve. In order for constitutive functions of the resulting theory to have nice symmetry conditions it is often convenient to take the base curve to be a curve of centroids of the 2- or 3-dimensional body (provided that this curve exists). On the other hand, for contact problems, it is most convenient to choose the base curve to lie on the boundary potentially in contact with the obstacle. In consequence, constitutive restrictions that are attractive in one formulation can be very complicated in another. Reconciling the resulting conflicts between different representations is one of the aims of this paper.

Deformation. Let $\{\boldsymbol{i},\boldsymbol{j},\boldsymbol{k}\}$ be a right-handed orthonormal basis for Euclidean 3-space. For simplicity, we restrict our attention to (time-independent) plane-strain deformations of a material body whose reference configuration is an infinite cylinder $\mathcal{B}\times\operatorname{span}\{\boldsymbol{k}\}$ with generators parallel to $\boldsymbol{k}$. Here $\mathcal{B}$ is a thin (curvilinear rectangular) region in the $\{\boldsymbol{i},\boldsymbol{j}\}$-plane that has the form

$$\mathcal{B} = \{\boldsymbol{r}^\circ(s) + x\boldsymbol{b}^\circ(s) : (s,x)\in\mathcal{Q}\}, \qquad \mathcal{Q} := \{(s,x) : s^- \le s \le s^+, h^-(s) \le x \le h^+(s)\} \tag{2.2}$$

where $s^\pm$ are given numbers, $h^\pm$ are given piecewise continuous functions for which $h^+(s) > h^-(s)$ for $s^- < s < s^+$, $\boldsymbol{r}^\circ$ and $\boldsymbol{b}^\circ$ are given continuous functions with piecewise continuous derivatives having values in span $\{\boldsymbol{i},\boldsymbol{j}\}$, $\boldsymbol{b}^\circ$ is a unit-vector-valued function, and the mapping

$$\mathcal{Q} \ni (s,x) \mapsto \boldsymbol{r}^\circ(s) + x\boldsymbol{b}^\circ(s)$$

is one-to-one. $\boldsymbol{r}^\circ$ is the *base curve* and the pair $\{\boldsymbol{r}^\circ, \boldsymbol{b}^\circ\}$ is the *skeleton* of $\mathcal{B}$. We restrict our attention to $\mathcal{Q}$'s for which $h^+ \geq 0 \geq h^-$.

We treat the special class of constrained deformations (2.1) of $\mathcal{B}$ that have the form

$$\boldsymbol{\varphi}(\mathbf{x}) = \boldsymbol{p}(s,x) + y\boldsymbol{k} = \boldsymbol{r}(s) + x\boldsymbol{b}(s) + y\boldsymbol{k}, \quad (s,x) \in \mathcal{Q}, \quad y \in \mathbb{R}, \tag{2.3}$$

where the functions $\boldsymbol{r}$ and $\boldsymbol{b}$ are absolutely continuous functions with values in span $\{\boldsymbol{i},\boldsymbol{j}\}$, with $\boldsymbol{b}$ a unit-vector-valued function. (Absolutely continuous functions, which have an (ε,δ)-definition, are exactly those functions that are indefinite integrals of (Lebesgue) integrable functions. Absolutely continuous functions have derivatives a.e.) The deformation is thus determined by the functions $\boldsymbol{r}$ and $\boldsymbol{b}$ (which here constitute the $\mathbf{u}$ of (2.1)). $\boldsymbol{r}$ gives the deformed image of the base curve $\boldsymbol{r}^\circ$ and $\boldsymbol{b}(s)$ gives the deformed orientation of the section determined by $\boldsymbol{b}^\circ(s)$.

We denote the values of functions in the reference configuration by subscripted or superscripted circles. If u is any such function, then $u_\circ = u^\circ$ (so that other indices can be conveniently attached to u).

We set $\boldsymbol{a} := -\boldsymbol{k} \times \boldsymbol{b}$ and let θ denote the angle from $\boldsymbol{i}$ to $\boldsymbol{a}$, so that

$$\boldsymbol{a} = \cos\theta\boldsymbol{i} + \sin\theta\boldsymbol{j}, \quad \boldsymbol{b} = -\sin\theta\boldsymbol{i} + \cos\theta\boldsymbol{j}. \tag{2.4}$$

Thus a configuration can be alternatively described by the pair $(\boldsymbol{r},\theta)$.

We denote differentiation with respect to s by a prime and differentiation with respect to other variables by subscripts. We set

$$\boldsymbol{r}' =: \nu\boldsymbol{a} + \eta\boldsymbol{b}, \quad \mu := \theta'. \tag{2.5}$$

The functions ν,η,μ, integrable on $[s^-,s^+]$ by virtue of the absolute continuity of $\boldsymbol{r}$ and $\boldsymbol{b}$, are the strains for our problem. They determine a configuration $(\boldsymbol{r},\theta)$ to within a rigid displacement.

Let $\mathcal{S}$ consist of those $s \in [s^-,s^+]$ at which $\boldsymbol{r}$ and θ are differentiable, and let

$$\mathcal{Q}(s) := \{x : h^-(s) \leq x \leq h^+(s)\}. \tag{2.6}$$

We require that (2.3) locally preserve orientation in the sense that its Jacobian

$$[\boldsymbol{\varphi}_s(\mathbf{x}) \times \boldsymbol{\varphi}_x(\mathbf{x})] \cdot \boldsymbol{\varphi}_y(\mathbf{x}) \equiv \boldsymbol{k} \cdot [(\boldsymbol{r}'(s) - x\theta'(s)\boldsymbol{a}(s)) \times \boldsymbol{b}(s)] \equiv \nu(s) - x\mu(s) > 0 \tag{2.7}$$

for all $s \in \mathcal{S}$ and for all $x \in \mathcal{Q}(s)$. This restriction is equivalent to

$$\nu(s) > \begin{cases} h^+(s)\mu(s) & \text{for} \quad \mu(s) \geq 0, \\ h^-(s)\mu(s) & \text{for} \quad \mu(s) \leq 0 \end{cases} \tag{2.8}$$

for all $s \in \mathcal{S}$. In particular, we require that (2.8) hold in the reference configuration, for which $\mathcal{S}^\circ$ consists of $[s^-,s^+]$ except for a finite number of points. (Our restrictions on the signs of $h^\pm$ ensure that $\nu > 0$ a.e.)

Let

$$\tilde{\boldsymbol{z}}(s,x,y) := \boldsymbol{\varphi}^\circ(\mathbf{x}) \equiv \boldsymbol{r}^\circ(s) + x\boldsymbol{b}^\circ(s) + y\boldsymbol{k} \equiv \boldsymbol{p}^\circ(s,x) + y\boldsymbol{k}. \tag{2.9}$$

Denote the inverse of $\tilde{\boldsymbol{z}}$ by $\boldsymbol{z} \mapsto (\tilde{s}(\boldsymbol{z}), \tilde{x}(\boldsymbol{z}), \tilde{y}(\boldsymbol{z}))$. The Inverse-Function Theorem implies that

$$\boldsymbol{I} = \frac{\partial\tilde{\boldsymbol{z}}}{\partial s}\frac{\partial\tilde{s}}{\partial\boldsymbol{z}} + \frac{\partial\tilde{\boldsymbol{z}}}{\partial x}\frac{\partial\tilde{x}}{\partial\boldsymbol{z}} + \frac{\partial\tilde{\boldsymbol{z}}}{\partial y}\frac{\partial\tilde{y}}{\partial\boldsymbol{z}} = [(\nu^\circ - x\mu^\circ)\boldsymbol{a}^\circ + \eta^\circ\boldsymbol{b}^\circ]\frac{\partial\tilde{s}}{\partial\boldsymbol{z}} + \boldsymbol{b}^\circ\frac{\partial\tilde{x}}{\partial\boldsymbol{z}} + \boldsymbol{k}\frac{\partial\tilde{y}}{\partial\boldsymbol{z}} \tag{2.10}$$

where $\boldsymbol{I}$ is the identity. By successively premultiplying this equation with $\boldsymbol{a}^\circ\cdot$, $\boldsymbol{b}^\circ\cdot$, $\boldsymbol{k}\cdot$, we obtain

$$\tilde{s}_{\boldsymbol{z}} = (\nu^\circ - x\mu^\circ)^{-1}\boldsymbol{a}^\circ, \quad \tilde{x}_{\boldsymbol{z}} = \boldsymbol{b}^\circ - \eta^\circ(\nu^\circ - x\mu^\circ)^{-1}\boldsymbol{a}^\circ, \quad \tilde{y}_{\boldsymbol{z}} = \boldsymbol{k}. \tag{2.11}$$

Thus the (transposed) deformation gradient is

$$\boldsymbol{F} = \frac{\partial \boldsymbol{p}}{\partial s}\frac{\partial \tilde{s}}{\partial \boldsymbol{z}} + \frac{\partial \boldsymbol{p}}{\partial x}\frac{\partial \tilde{x}}{\partial \boldsymbol{z}} + \boldsymbol{k}\boldsymbol{k} \equiv [(\nu - x\mu)\boldsymbol{a} + (\eta - \eta^\circ)\boldsymbol{b}]\frac{\boldsymbol{a}^\circ}{\nu^\circ - x\mu^\circ} + \boldsymbol{b}\boldsymbol{b}^\circ + \boldsymbol{k}\boldsymbol{k}. \tag{2.12}$$

Note that (2.7) ensures that the denominator $\nu^\circ - x\mu^\circ$ cannot vanish for $s \in \mathcal{S}^\circ$. The right Cauchy-Green deformation tensor is

$$\boldsymbol{C} = \boldsymbol{F}^* \cdot \boldsymbol{F} = [(\nu - x\mu)^2 + (\eta - \eta^\circ)^2]\frac{\boldsymbol{a}^\circ\boldsymbol{a}^\circ}{(\nu^\circ - x\mu^\circ)^2} + (\eta - \eta^\circ)\frac{\boldsymbol{a}^\circ\boldsymbol{b}^\circ + \boldsymbol{b}^\circ\boldsymbol{a}^\circ}{\nu^\circ - x\mu^\circ} + \boldsymbol{b}^\circ\boldsymbol{b}^\circ + \boldsymbol{k}\boldsymbol{k}. \tag{2.13}$$

Equilibrium. Let $\boldsymbol{T}(\boldsymbol{z})$ denote the first Piola-Kirchhoff stress tensor at $\boldsymbol{z}$, let $\boldsymbol{\gamma}(\boldsymbol{p}^\circ(s,x), \boldsymbol{p}(s,x))$ denote the body force per unit reference volume at $\mathbf{x}$, and let $\boldsymbol{\tau}^\pm(\boldsymbol{p}^\circ(s,x), \boldsymbol{p}(s,x))$ denote the tractions per unit reference surface area on the top and bottom of the body at $\mathbf{x}$. (The possible dependence of these functions on the actual position accommodates live loads. A slight generalization is needed to account for hydrostatic pressure.) We suppose that $\boldsymbol{T}$, $\boldsymbol{\gamma}$, $\boldsymbol{\tau}^\pm$ are independent of y. If we take the virtual displacements $\boldsymbol{p}_\vartriangle$ to be consistent with (2.3) (i.e., if we take them to be in the tangent space to the constraint manifold of (2.3)):

$$\boldsymbol{p}_\vartriangle = \boldsymbol{r}_\vartriangle - x\theta_\vartriangle\boldsymbol{a}, \tag{2.14}$$

then the Principle of Virtual Work (or weak formulation of the equilibrium equations) [1, Chap. 14] implies that

$$\begin{aligned} &\int_Q \{[\boldsymbol{T}\cdot\boldsymbol{a}^\circ]\cdot[\boldsymbol{r}_\vartriangle{}' - x(\theta_\vartriangle{}'\boldsymbol{a} + \theta_\vartriangle\theta'\boldsymbol{b})] - [\boldsymbol{T}\cdot\boldsymbol{b}^\circ]\cdot[\theta_\vartriangle\boldsymbol{a}] + \boldsymbol{\gamma}\cdot[\boldsymbol{r}_\vartriangle - x\theta_\vartriangle\boldsymbol{a}](\nu^\circ - x\mu^\circ)\}\,dx\,ds \\ &+ \int_{s^-}^{s^+} \boldsymbol{\tau}^+\cdot[\boldsymbol{r}_\vartriangle - h^+\theta_\vartriangle\boldsymbol{a}]\,|\tfrac{d}{ds}[\boldsymbol{r}^\circ + h^+\boldsymbol{b}^\circ]|\,ds - \int_{s^-}^{s^+} \boldsymbol{\tau}^-\cdot[\boldsymbol{r}_\vartriangle - h^-\theta_\vartriangle\boldsymbol{a}]\,|\tfrac{d}{ds}[\boldsymbol{r}^\circ + h^-\boldsymbol{b}^\circ]|\,ds = 0 \end{aligned} \tag{2.15}$$

for all $\boldsymbol{r}_\vartriangle$ and $\theta_\vartriangle$ vanishing at $s^\pm$. Let us set

$$\boldsymbol{n} := \int_{h^-}^{h^+} \boldsymbol{T}\cdot\boldsymbol{a}^\circ\,dx, \tag{2.16}$$

$$M := -\boldsymbol{a}\cdot\int_{h^-}^{h^+} x\boldsymbol{T}\cdot\boldsymbol{a}^\circ\,dx, \tag{2.17}$$

$$\boldsymbol{f} := \int_{h^-}^{h^+} \boldsymbol{\gamma}(\nu^\circ - x\mu^\circ)\,dx + \boldsymbol{\tau}^+|\tfrac{d}{ds}[\boldsymbol{r}^\circ + h^+\boldsymbol{b}^\circ]| - \boldsymbol{\tau}^-|\tfrac{d}{ds}[\boldsymbol{r}^\circ + h^-\boldsymbol{b}^\circ]|, \tag{2.18}$$

$$l := -\boldsymbol{a}\cdot\int_{h^-}^{h^+} x\boldsymbol{\gamma}(\nu^\circ - x\mu^\circ)\,dx - \boldsymbol{a}\cdot\boldsymbol{\tau}^+|\tfrac{d}{ds}[\boldsymbol{r}^\circ + h^+\boldsymbol{b}^\circ]|h^+ - \boldsymbol{a}\cdot\boldsymbol{\tau}^-|\tfrac{d}{ds}[\boldsymbol{r}^\circ + h^-\boldsymbol{b}^\circ]|h^-. \tag{2.19}$$

$\boldsymbol{n}(s)$ is the resultant contact force across the section at s, M is the resultant contact couple across the section at s, $\boldsymbol{f}(s)$ is the external force exerted at s per unit of s, and $l(s)$ is the external couple exerted at s per unit of s. Then (2.15) is equivalent to a simpler version involving these new rod-theoretic variables. If the functions entering this formulation are sufficiently smooth, then the use of symmetry condition for $\boldsymbol{T}$ shows that this formulation is equivalent to the classical equilibrium equations [1, Chap. 14]

$$\boldsymbol{n}' + \boldsymbol{f} = \boldsymbol{0}, \tag{2.20}$$

$$M' + \boldsymbol{k} \cdot (\boldsymbol{r}' \times \boldsymbol{n}) + l = 0. \tag{2.21}$$

We set

$$\boldsymbol{n} = N\boldsymbol{a} + H\boldsymbol{b}, \tag{2.22}$$

from which we get componential forms of (2.20) and (2.21):

$$N' - \mu H + \boldsymbol{f} \cdot \boldsymbol{a} = 0, \quad H' + \mu N + \boldsymbol{f} \cdot \boldsymbol{b} = 0, \quad M' + \nu H - \eta N + l = 0. \tag{2.23}$$

Constitutive equations. We get constitutive equations for the resultants N, H, M from (2.16) and (2.17) by replacing the $\boldsymbol{T}$ there with its constitutive function. In particular, elastic materials have constitutive equations of the form

$$\boldsymbol{T} = \hat{\boldsymbol{T}}(\boldsymbol{F}, \boldsymbol{z}) = \boldsymbol{F} \cdot \hat{\boldsymbol{S}}(\boldsymbol{C}, \boldsymbol{z}) \tag{2.24}$$

where $\hat{\boldsymbol{S}}$ is the symmetric second Piola-Kirchhoff stress tensor. The substitution of (2.12) and (2.13) into (2.24) shows that the constitutive functions for N, H, M depend only on the strains ν, η, μ:

$$N(s) = \hat{N}(\nu(s), \eta(s), \mu(s), s), \quad \text{etc.} \tag{2.25}$$

We assume that the reference configuration is natural, i.e., stress-free, so that $\hat{\boldsymbol{T}}(\boldsymbol{I}, \boldsymbol{z}) = \boldsymbol{O}$ and

$$\hat{N}(\nu^\circ(s), \eta^\circ(s), \mu^\circ(s), s) = 0, \quad \text{etc.} \tag{2.26}$$

For simplicity of exposition, we assume that $\hat{N}, \hat{H}, \hat{M}$ are continuously differentiable. (By replacing our differential equations with integral equations, we could still carry out most of our analysis under far weaker assumptions.)

If $\hat{\boldsymbol{T}}$ satisfies the strict form of the Strong Ellipticity Condition, then it can be shown [1, Chap. 14] that $(\hat{N}, \hat{H}, \hat{M})$ satisfies the *strict monotonicity condition*:

$$\begin{bmatrix} \hat{N}_\nu & \hat{N}_\eta & \hat{N}_\mu \\ \hat{H}_\nu & \hat{H}_\eta & \hat{H}_\mu \\ \hat{M}_\nu & \hat{M}_\eta & \hat{M}_\mu \end{bmatrix} \quad \text{is positive-definite.} \tag{2.27}$$

We assume that this condition holds throughout this paper. If $\hat{\boldsymbol{S}}$ has the usual symmetry with respect to the shear components of $\boldsymbol{C}$, and if $\eta^\circ = 0$ (cf. (3.1)), then it can be shown [1, Sec. 14.4] that

$$\hat{N}(\nu, \cdot, \mu, s) \quad \text{and} \quad \hat{M}(\nu, \cdot, \mu, s) \quad \text{are even,} \quad \hat{H}(\nu, \cdot, \mu, s) \quad \text{is odd.} \tag{2.28}$$

If $\eta^\circ = 0$ and $\mu^\circ = 0$ (so that the base curve $\boldsymbol{r}^\circ$ is a straight line) and if $\boldsymbol{r}^\circ$ is a line of centroids, then it can be shown [1, Sec. 14.5] that

$$\hat{N}(\nu, \eta, \cdot, s) \quad \text{and} \quad \hat{H}(\nu, \eta, \cdot, s) \quad \text{are even,} \quad \hat{M}(\nu, \eta, \cdot, s) \quad \text{is odd.} \tag{2.29}$$

If

$$[\nu \hat{H}(\nu, \eta, \mu, s) - \eta \hat{N}(\nu, \eta, \mu, s)]\eta > 0 \quad \text{for all } (\nu, \eta, \mu, s) \text{ with } \eta \neq 0, \tag{2.30}$$

then rods cannot suffer shear instabilities of the sort described in [1, Chap. 5].

If both the strict monotonicity condition(2.27) and the *coercivity* condition

$$\begin{aligned} &|\hat{N}(\nu, \eta, \mu, s)| + |\hat{H}(\nu, \eta, \mu, s)| + |\hat{N}(\nu, \eta, \mu, s)| \to \infty \\ &\qquad\qquad \text{as} \quad |\nu| + |\eta| + |\mu| \to \infty \quad \text{or as} \quad \nu - V(\mu, s) \to 0, \end{aligned} \tag{2.31}$$

hold, then it can be shown [1, Chap. 9] that there are inverse constitutive functions $\hat{\nu}, \hat{\eta}, \hat{\mu}$ such that (2.25) is equivalent to

$$\nu(s) = \hat{\nu}(N(s), H(s), M(s), s), \quad \text{etc.} \tag{2.32}$$

These inverse functions are also strictly monotone, and inherit the smoothness, symmetry, and appropriate coercivity properties of (2.25). Henceforth, we simply assume that (2.25) and (2.32) are equivalent.

This sketch of the theory of shearable rods suppresses subtle questions associated with the Lagrange multipliers that maintain the constraint (2.3) and that are responsible for the effectiveness of the governing equations, by ensuring, e.g., that the traction boundary conditions on the lateral surface of the rod are identically satisisfied. See [1, Chap. 14] for details.

3 Transformation of the base curve

It is usually convenient to take the reference configuration to be a natural configuration in which the contact forces and couples vanish. It is customary to assume that in this configuration, s is the arc-length parameter for the curve $\boldsymbol{r}^\circ$ and, more importantly, that $\boldsymbol{b}^\circ$ is orthogonal to $\boldsymbol{r}_\circ'$. In this case,

$$\nu^\circ = 1, \quad \eta^\circ = 0, \quad \text{i.e.,} \quad \boldsymbol{r}_\circ' = \boldsymbol{a}_\circ, \tag{3.1}$$

and the curvature of $\boldsymbol{r}^\circ$ is μ°. If $\boldsymbol{r}^\circ$ is taken to be the curve of centroids of $\mathcal{B}$, provided that this curve exists, then the constitutive equations typically are as simple as possible and enjoy various symmetries. A trivial example of the nonexistence of a curve of centroids is that for a body of the form $\{s\boldsymbol{i} + x\boldsymbol{j} : -1 \le s \le 1, 0 \le x \le h^+(s)\}$ where $h^+(s) = \alpha > 0$ for $s < 0$ and $= \beta > 0$ for $s \ge 0$ with $\alpha \ne \beta$. By abandoning the requirement that the curve of centroids be continuous (and thus by abandoning the requirement that it be a curve), we could immediately exhibit two straight-line segments that would serve as curves of centroids for the left and right parts of this body, and would give a representation simplifying the constitutive equations. Below we exhibit quite simple geometries with continuous $h^\pm$ for which it is unlikely that a curve of centroids exists. (Many of the virtues of the curve of centroids evaporate for dynamical problems, as we point out in the Conclusion.) For contact problems, it is more convenient to take $\boldsymbol{r}^\circ$ to be a bounding curve of $\mathcal{B}$ that could come into contact with obstacles. This section is devoted to the problem of determining when rod theories based upon different choices of $(\boldsymbol{r}^\circ, \boldsymbol{b}^\circ)$ are equivalent in a sense to be made precise.

Before beginning our analysis, it is illuminating to consider a simple example, that of the body $\mathcal{B}$ shown in Figure 1a. The top of $\mathcal{B}$ is the arc of the circle of radius 1 centered at the origin $\boldsymbol{0}$ and subtending an angle $\frac{\pi}{2}$ in going from $-\boldsymbol{j}$ to $\boldsymbol{i}$. The bottom of $\mathcal{B}$ is the arc of the circle of radius $\sqrt{5}$ centered at $\boldsymbol{j}$ and subtending an angle $\arctan 2$ in going from $-(\sqrt{5}-1)\boldsymbol{j}$ to $2\boldsymbol{i}$. The left end is the straight line joining $-\boldsymbol{j}$ to $-(\sqrt{5}-1)\boldsymbol{j}$ and the right end is the straight line joining $\boldsymbol{i}$ to $2\boldsymbol{i}$. There are many choices for $(\boldsymbol{r}^\circ, \boldsymbol{b}^\circ)$; we discuss just five, which are distinguished by the subscripts 1, ... ,5 attached to the functions defining $\mathcal{B}$:

(1) If the top were subject to contact, we would be motivated to take it as the base curve $\boldsymbol{r}_1^\circ$ parametrized, e.g., by the angle ϕ from $-\boldsymbol{j}$ to the position vector on the top circle:

$$[0, \tfrac{\pi}{2}] \ni \phi \mapsto \boldsymbol{r}_1^\circ(\phi) := \sin\phi\boldsymbol{i} - \cos\phi\boldsymbol{j} \tag{3.2}$$

and we could choose $\boldsymbol{b}_1^\circ$ to be the unit normal field to this circle:

$$[0, \tfrac{\pi}{2}] \ni \phi \mapsto \boldsymbol{b}_1^\circ(\phi) := -\sin\phi\boldsymbol{i} + \cos\phi\boldsymbol{j}. \tag{3.3}$$

Here ϕ is the arc-length parameter. In this case, (3.1) would hold. The requirement that x measure distance from $\boldsymbol{r}^\circ$ along $\boldsymbol{b}^\circ$ fixes $h_1^\pm$, so that $h_1^+(\phi) = 0$. To find $h_1^-(\phi)$ we must parametrize the bottom curve by ϕ; we first parametrize it by the angle ψ between the downward vertical from $\boldsymbol{j}$ and the ray from $\boldsymbol{j}$ to a point on the bottom circle:

$$[0, \arctan 2] \ni \psi \mapsto \boldsymbol{j} + \sqrt{5}[\sin\psi\boldsymbol{i} - \cos\psi\boldsymbol{j}]. \tag{3.4}$$

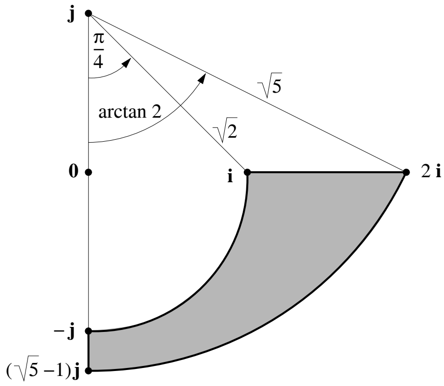

Figure 1a. The body $\mathcal{B}$. Different skeletons for it are shown in Figures 1b–1f.

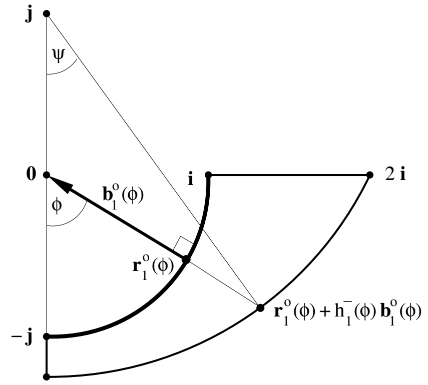

Figure 1b. The (thick) top curve is the base curve. It and the cross sections orthogonal to it form the skeleton.

We equate this expression to the representation of the bottom circle in terms of the parameter ϕ:

$$[0, \tfrac{\pi}{2}] \ni \phi \mapsto \boldsymbol{r}_1^\circ(\phi) + h_1^-(\phi)\boldsymbol{b}_1^\circ(\phi) = [1 - h_1^-(\phi)][\sin\phi\,\boldsymbol{i} - \cos\phi\,\boldsymbol{j}], \tag{3.5}$$

from which we obtain

$$h_1^-(\phi) = 1 + \cos\phi - \sqrt{4 + \cos^2\phi}. \tag{3.6}$$

(See Figure 1b.)

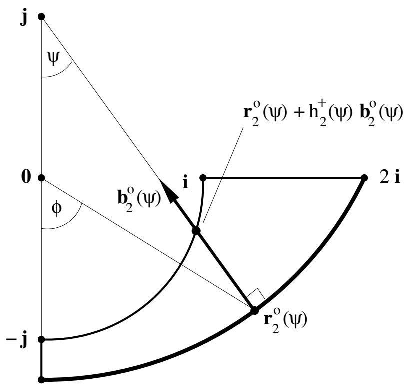

Figure 1c. The (thick) bottom curve is the base curve. It and the cross sections orthogonal to it form the skeleton.

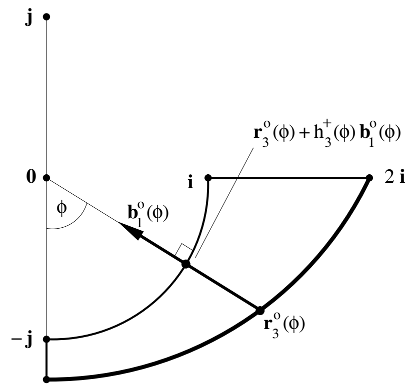

Figure 1d. The (thick) bottom curve is the base curve. It and the sections orthogonal to the *top* form the skeleton.

(2) If the bottom were subject to contact, we would be motivated to take it as the base curve $\boldsymbol{r}_2^\circ$. Then we could describe it by (3.4). (We could replace ψ with an arc-length parameter $s = \sqrt{5}\psi$.) We could take $\boldsymbol{b}_2^\circ$ to be the unit normal field to (3.4), given by $\boldsymbol{k} \times (\boldsymbol{r}_2^\circ)'/|(\boldsymbol{r}_2^\circ)'|$. In this case, if the arc-length

parametrization were used, then (3.1) would hold. The $h_2^{\pm}$ as functions of ψ are determined as in case (i) by the equation $\boldsymbol{r}_2^\circ(\psi) + h_2^+(\psi)\boldsymbol{b}_2^\circ(\psi) = \sin\phi\boldsymbol{i} - \cos\phi\boldsymbol{j}$:

$$h_2^-(\psi) = 0, \quad h_2^+(\psi) = \sqrt{5} - \begin{cases} 2\cos\psi & \text{for } \ 0 \le \psi \le \frac{\pi}{4}, \\ \sec\psi & \text{for } \ \frac{\pi}{4} \le \psi \le \arctan 2. \end{cases} \tag{3.7}$$

(See Figure 1c.)

(3) Alternatively, we could take the bottom as the base curve $\boldsymbol{r}_3^\circ$ parametrized with ϕ by (3.5), (3.6). In this case, we could use (3.3) to define $\boldsymbol{b}_3^\circ := \boldsymbol{b}_1^\circ$, but $\boldsymbol{b}_3^\circ$ would not be orthogonal to $\boldsymbol{r}_3^\circ$, so that (3.1) would not hold. (See Figure 1d.)

(4), (5) Since it is unlikely that $\mathcal{B}$ admits a (globally defined) curve of centroids in the traditional sense of bisecting normal sections to itself, we could take the sections to be determined, e.g., by $\boldsymbol{b}_1^\circ$ or $\boldsymbol{b}_2^\circ$ and find the corresponding curves $\boldsymbol{r}_4^\circ$ or $\boldsymbol{r}_5^\circ$ bisecting these sections:

$$\boldsymbol{r}_4^\circ := [1 - \tfrac{1}{2}h_1^-(\phi)][\sin\phi\boldsymbol{i} - \cos\phi\boldsymbol{j}], \tag{3.8}$$

$$\boldsymbol{r}_5^\circ := \boldsymbol{j} + [\sqrt{5} - \tfrac{1}{2}h_2^+(\psi)][\sin\psi\boldsymbol{i} - \cos\psi\boldsymbol{j}]. \tag{3.9}$$

(See Figures 1e,f.) In these cases (3.1) would not hold and we could not expect the constitutive equations

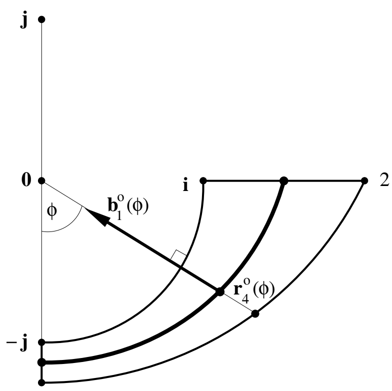

Figure 1e. The (thick) curve of centroids is the base curve. It and the sections orthogonal to the top curve form the skeleton.

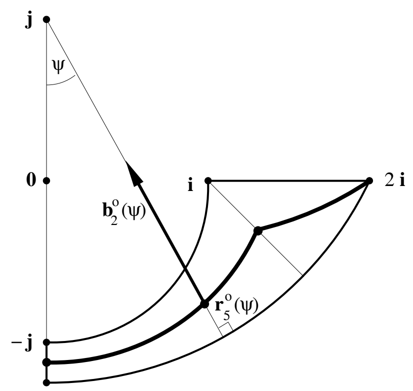

Figure 1f. The (thick) curve of centroids is again the base curve. It and the sections orthogonal to the bottom curve form the skeleton.

to have nice symmetry properties. The difficulties of using some semblance of a curve of centroids as a base curve might prompt us to take either the top or bottom circle as base curve, even when there is no question of contact.

We now determine when different choices of $(\boldsymbol{r}^\circ, \boldsymbol{b}^\circ)$ lead to equivalent theories. Let $(\boldsymbol{r}_1^\circ, \boldsymbol{b}_1^\circ)$ and $(\boldsymbol{r}_2^\circ, \boldsymbol{b}_2^\circ)$ be two different skeletons for $\mathcal{B}$ satisfying (2.7) (which is equivalent to (2.8)), so that $\mathcal{B}$ has alternative and equivalent parametrizations (s_1, x_1) and (s_2, x_2) such that

$$\{\boldsymbol{r}_1^\circ(s_1) + x_1\boldsymbol{b}_1^\circ(s_1) : (s_1, x_1) \in \mathcal{Q}_1\} = \{\boldsymbol{r}_2^\circ(s_2) + x_2\boldsymbol{b}_2^\circ(s_2) : (s_2, x_2) \in \mathcal{Q}_2\}. \tag{3.10}$$

(cf. (2.2)). The equivalence of these parametrizations means that the equation

$$\boldsymbol{r}_1^\circ(s_1) + x_1\boldsymbol{b}_1^\circ(s_1) = \boldsymbol{r}_2^\circ(s_2) + x_2\boldsymbol{b}_2^\circ(s_2) \tag{3.11}$$

for $(s_1, x_1) \in \mathcal{Q}_1$ can be uniquely solved for s_2, x_2:

$$s_2 = \hat{s}_2(s_1, x_1), \quad x_2 = \hat{x}_2(s_1, x_1), \tag{3.12}$$

and vice versa:

$$s_1 = \hat{s}_1(s_2, x_2), \quad x_1 = \hat{x}_1(s_2, x_2). \tag{3.13}$$

By exploiting (3.10) and the fact that the $\boldsymbol{b}^\circ$ are independent of x, we could obtain certain restrictions on the $\boldsymbol{b}^\circ$'s and $h^\pm$'s. We do not pause to work out the details of this observation because we can get much sharper necessary restrictions by imposing the definition that two rod theories based on (2.3) and (2.2) are *geometrically equivalent* if they admit exactly the same set of deformations. In particular, if $\boldsymbol{p}_1$ and $\boldsymbol{p}_2$ are deformations respectively generated by $(\boldsymbol{r}_1, \boldsymbol{b}_1)$ and $(\boldsymbol{r}_2, \boldsymbol{b}_2)$ via (2.3), then they admit the same set of deformations if for any given absolutely continuous $(\boldsymbol{r}_1, \boldsymbol{b}_1)$ satisfying (2.7), the equation

$$\boldsymbol{p}_1(\hat{s}_1(s_2, x_2), \hat{x}_1(s_2, x_2)) = \boldsymbol{p}_2(s_2, x_2), \qquad (s_2, x_2) \in \mathcal{Q}_2, \tag{3.14}$$

can be uniquely solved for absolutely continuous $(\boldsymbol{r}_2, \boldsymbol{b}_2)$ (satisfying (2.7)) in terms of $(\boldsymbol{r}_1, \boldsymbol{b}_1)$ and vice versa. Note that this equivalence ensures that (3.11) holds.

We first determine necessary conditions for equivalence: We choose $\boldsymbol{p}_1$ to be a deformation that straightens the axis of the rod, stretches it, and reduces the shear to 0:

$$\boldsymbol{p}_1(s_1, x_1) = cs_1\boldsymbol{i} + x_1\boldsymbol{j} \tag{3.15}$$

where c is a positive constant. Note that (3.15) can be effected by a continuous 1-parameter family of deformations from the reference configuration each of which, including (3.15) satisfies(2.7). Then (3.14) implies that

$$\boldsymbol{r}_2(s_2) + x_2\boldsymbol{b}_2(s_2) = c\hat{s}_1(s_2, x_2)\boldsymbol{i} + \hat{x}_1(s_2, x_2)\boldsymbol{j}. \tag{3.16}$$

Taking the dot products of (3.16) with $\boldsymbol{i}$ and $\boldsymbol{j}$, we see that $\hat{s}_1$ and $\hat{x}_1$ are affine functions of x_2, i.e., there are functions $\alpha, \beta, \gamma, \delta$ such that

$$\hat{x}_1(s_2, x_2) = \alpha(s_2)x_2 + \beta(s_2), \quad \hat{s}_1(s_2, x_2) = \gamma(s_2)x_2 + \delta(s_2). \tag{3.17}$$

Since $\hat{s}_1$ and $\hat{x}_1$ characterize the reference configuration, the functions $\alpha, \beta, \gamma, \delta$ cannot depend on the parameter c. Substituting (3.17) into (3.16) and using the arbitrariness of x_2, we obtain that

$$\boldsymbol{b}_2(s_2) = c\gamma(s_2)\boldsymbol{i} + \alpha(s_2)\boldsymbol{j}, \quad \boldsymbol{a}_2(s_2) = \boldsymbol{b}_2(s_2) \times \boldsymbol{k} = \alpha(s_2)\boldsymbol{i} - c\gamma(s_2)\boldsymbol{j}, \tag{3.18}$$

with

$$\alpha^2 + c^2\gamma^2 = 1 \tag{3.19}$$

because $\boldsymbol{a}_2$ and $\boldsymbol{b}_2$ are unit vectors. Since this equation must hold for all positive c it follows that $\gamma = 0$ and $\alpha = \pm 1$. We fix orientation by taking $\alpha = 1$, so that $\boldsymbol{a}_2 = \boldsymbol{i}$, $\boldsymbol{b}_2 = \boldsymbol{j}$. Thus (3.17) reduces to

$$\hat{x}_1(s_2, x_2) = x_2 + \beta(s_2), \quad \hat{s}_1(s_2, x_2) = \delta(s_2). \tag{3.20}$$

Now we substitute (3.20) into (3.11) to obtain

$$\boldsymbol{r}_1^\circ(\delta(s_2)) + [x_2 + \beta(s_2)]\boldsymbol{b}_1^\circ(\delta(s_2)) = \boldsymbol{r}_2^\circ(s_2) + x_2\boldsymbol{b}_2^\circ(s_2). \tag{3.21}$$

The arbitrariness of x_2 then implies necessary conditions for geometric equivalence: There exist functions β and δ such that $\mathcal{Q}_2$ can be transformed into $\mathcal{Q}_1$ by (3.20) and such that

$$\boldsymbol{b}_1^\circ(\delta(s_2)) = \boldsymbol{b}_2^\circ(s_2), \tag{3.22}$$

$$\boldsymbol{r}_1^\circ(\delta(s_2)) + \beta(s_2)\boldsymbol{b}_1^\circ(\delta(s_2)) = \boldsymbol{r}_2^\circ(s_2). \tag{3.23}$$

Condition (3.22) says that the $\boldsymbol{b}^\circ$ fields must be the same.

By differentiating of (3.22) and (3.23) we find that β and δ are differentiable a.e. We substitute (3.20) into (3.16), differentiate the resulting equation with respect to s_2, and take into account (3.18) to get

$$\mu_2(s_2) = 0, \quad \nu_2(s_2)\boldsymbol{i} + \eta_2(s_2)\boldsymbol{j} = c\delta'(s_2)\boldsymbol{i} + \beta'(s_2)\boldsymbol{j}. \tag{3.24}$$

Consequently, β, δ have to be absolutely continuous (since ν_2, η_2 are integrable). Since $\nu_2(s_2) > 0$ a.e. by (2.8), we obtain the natural condition that $\delta'(s_2) > 0$ a.e., i.e., δ is increasing.

Since $\delta' > 0$ a.e., we can use (3.20) to show that the corner points $(s_1^-, h_1^-(s_1^-))$, $(s_1^-, h_1^+(s_1^-))$, $(s_1^+, h_1^-(s_1^+))$, $(s_1^+, h_1^+(s_1^+))$ of $\mathcal{Q}_1$ go into the corresponding corner points of $\mathcal{Q}_2$. (For this purpose, we note that $s_2^+ = \sup\{s_2 : (s_2, x_2) \in \mathcal{Q}_2\}$ and $h_2^+ = \sup\{x_2 \in \mathcal{Q}_2(s_2^+)\}$.

Now we study the preservation of orientation and absolute continuity under geometrically equivalent transformations. We assume that there are skeletons $(\boldsymbol{r}_1^\circ, \boldsymbol{b}_1^\circ)$, $(\boldsymbol{r}_2^\circ, \boldsymbol{b}_2^\circ)$ satisfying (2.7) and that there are absolutely continuous functions β and δ with $\delta'(s_2) > 0$ a.e. on $[s_2^-, s_2^+]$ such that $\mathcal{Q}_2$ transforms into $\mathcal{Q}_1$ acccording to (3.20) and such that (3.22) and (3.23) hold. Our study of the transformation of the strains will show that our necessary conditions are also sufficient for geometric equivalence and will be useful in our study of constitutive equations. We substitute (3.20) into (3.14) to obtain

$$\boldsymbol{r}_2(s_2) + x_2\boldsymbol{b}_2(s_2) = \boldsymbol{r}_1(\delta(s_2)) + [x_2 + \beta(s_2)]\boldsymbol{b}_1(\delta(s_2)) \tag{3.25}$$

and immediately obtain, just as for (3.22) and (3.23), that

$$\boldsymbol{b}_1(\delta(s_2)) = \boldsymbol{b}_2(s_2), \tag{3.26}$$

$$\boldsymbol{r}_1(\delta(s_2)) + \beta(s_2)\boldsymbol{b}_1(\delta(s_2)) = \boldsymbol{r}_2(s_2). \tag{3.27}$$

Thus a unique pair $(\boldsymbol{r}_2, \boldsymbol{b}_2)$ is assigned to each deformation $(\boldsymbol{r}_1, \boldsymbol{b}_1)$. Conversely, with the inverse transformation of (3.20) given by

$$\hat{s}_2(s_1, x_1) = \delta^{-1}(s_1), \quad \hat{x}_2(s_1, x_1) = x_1 - \beta(\delta^{-1}(s_1)) \tag{3.28}$$

we can use analogous arguments to show that a unique pair $(\boldsymbol{r}_1, \boldsymbol{b}_1)$ can be associated with each $(\boldsymbol{r}_2, \boldsymbol{b}_2)$. Note that (3.26) and (3.27) also imply (3.22) and (3.23). To verify that the rod theories are geometrically equivalent we still have to show that $\boldsymbol{r}_2$ and $\boldsymbol{b}_2$ are absolutely continuous and that $(\boldsymbol{r}_2, \boldsymbol{b}_2)$ satisfies (2.7) if and only if the same is true for $(\boldsymbol{r}_1, \boldsymbol{b}_1)$.

Differentiating (3.26) with respect to s_2 we obtain

$$\mu_1(\delta(s_2))\delta'(s_2) = \mu_2(s_2). \tag{3.29}$$

Differentiating (3.27) with respect to s_2 we obtain

$$[\nu_1(\delta(s_2)) - \beta(s_2)\mu_1(\delta(s_2))]\delta'(s_2) = \nu_2(s_2), \tag{3.30}$$

$$\eta_1(\delta(s_2))\delta'(s_2) + \beta'(s_2) = \eta_2(s_2). \tag{3.31}$$

Since $\delta' > 0$ a.e., we can use the formula for changing variables in integrals to derive from (3.29) that

$$\int_{s_1^-}^{s_1^+} |\mu_1(s_1)|\, ds_1 = \int_{s_2^-}^{s_2^+} |\mu(\delta(s_2))|\delta'(s_2)\, ds_2 = \int_{s_2^-}^{s_2^+} |\mu_2(s_2)|\, ds_2. \tag{3.32}$$

(To show that this formula applies to absolutely continuous coordinate transformations it is necessary to extend the standard formula for Lipschitz continuous transformations. We tacitly use analogous results below.) Hence μ_1 is integrable if and only if μ_2 is. Analogously, we derive from (3.30), (3.31) that ν_1 and η_1 are integrable if and only if ν_2 and η_2 are respectively integrable. Thus $\boldsymbol{r}_1$ and $\boldsymbol{b}_1$ are absolutely continuous if and only if $\boldsymbol{r}_2$ and $\boldsymbol{b}_2$ are. Now (3.29), (3.30), and (3.20) imply that

$$\nu_2(s_2) - x_2\mu_2(s_2) = [\nu_1(\hat{s}_1(s_2,x_2)) - \hat{x}_1(s_2,x_2)\mu_1(\hat{s}_1(s_2,x_2))]\delta'(s_2). \tag{3.33}$$

Since $\delta'(s_2) > 0$ a.e., pairs $(\boldsymbol{r}_1, \boldsymbol{b}_1)$ and $(\boldsymbol{r}_2, \boldsymbol{b}_2)$ related by (3.26), (3.27) each satisfy (2.7) or neither satisfies (2.7). We conclude that both theories have the same repertoire of deformations. It follows that our necessary conditions are also sufficient for geometric equivalence.

We specialize (3.30) to the reference configuration to obtain a representation for δ':

$$\delta' = \frac{\nu_2^\circ}{\nu_1^\circ - \beta\mu_1^\circ} \tag{3.34}$$

(condition(2.7) implies that the denominator cannot vanish except at a finite number of points. Equation (3.34) leads to elegant variants of our transformation formulas:

$$\mu_1\nu_2^\circ = (\nu_1^\circ - \beta\mu_1^\circ)\mu_2, \tag{3.35}$$

$$(\nu_1 - \beta\mu_1)\nu_2^\circ = (\nu_1^\circ - \beta\mu_1^\circ)\nu_2, \tag{3.36}$$

$$\eta_1\nu_2^\circ + (\nu_1^\circ - \beta\mu_1^\circ)\beta' = (\nu_1^\circ - \beta\mu_1^\circ)\eta_2. \tag{3.37}$$

Note that these last three conditions deliver (3.20), (3.26), (3.27) to within a rigid motion. From (3.35), (3.36), (3.37) we immediately get dual relations by switching the indices 1 and 2 and by replacing β by $-\beta$. In particular, from (3.35) and its dual we obtain

$$\frac{\nu_2^\circ}{\nu_1^\circ - \beta\mu_1^\circ} = \frac{\nu_2^\circ + \beta\mu_2^\circ}{\nu_1^\circ} = \delta'. \tag{3.38}$$

These results show that rod theories based upon the skeletons shown in the Figures 1.b,d,e are equivalent, that those for Figures 1.c,f are equivalent, but none of the theories of the first set are equivalent to those of the second.

It is of interest to determine those transformations that are consistent with a stronger notion of equivalence that requires that the customary properties (3.1) be preserved. If we impose the requirement that $\eta_1^\circ = 0 = \eta_2^\circ$, then the specialization of (3.31) to the reference configuration immediately implies that $\beta(\cdot)$ is a constant β, leading to a strong restriction on (3.20). If we impose the requirement that $\nu_1^\circ = 1 = \nu_2^\circ$, then the specialization of (3.34) yields $\delta'(s_2) = 1/[1 - \beta\mu_2^\circ(s_2)]$, which of course fixes δ up to a translation.

Now we show that geometrically equivalent rod theories are *mechanically equivalent* in the sense that the equilibrium equations are equivalent. Let $\mathcal{Q}_1([s_1^-, s_1^*])$ denote the part of $\mathcal{Q}_1$ lying between the lines $s_1 = s_1^-$ and $s_1 = s_1^*$:

$$\mathcal{Q}_1([s_1^-, s_1^*]) := \{(s_1, x_1) \in \mathcal{Q}_1 : s_1^- \le s_1 \le s_1^*\}. \tag{3.39}$$

$\mathcal{Q}_2([s_2^-, s_2^*])$ is defined analogously. For brevity, let us assume that $\boldsymbol{\tau}^\pm = \boldsymbol{0}$. We assume that the deformation of $\mathcal{B}$ is described by geometrically equivalent theories indexed by 1 and 2, so that (3.17)–(3.37) hold.

Then (2.19) implies that the total external couple on the part of $\mathcal{B}$ corresponding to $\mathcal{Q}_1([s_1^-, s_1^*])$ is

$$\begin{aligned} &\int_{s_1^-}^{s_1^*} l_1(s_1)\,ds_1 \\ &= -\int_{s_1^-}^{s_1^*}\int_{h_1^-(s_1)}^{h_1^+(s_1)} [x_1\,\boldsymbol{a}_1(s_1)\cdot\boldsymbol{\gamma}\big(\boldsymbol{r}_1{}^\circ(s_1) + x_1\,\boldsymbol{b}_1^\circ(s_1), \boldsymbol{r}_1(s_1) + x_1\,\boldsymbol{b}_1(s_1)\big)(\nu_1^\circ - x_1\mu_1^\circ)]\,dx_1\,ds_1. \end{aligned} \tag{3.40}$$

Under the change of variables (3.20) this integral becomes

(3.41)
$$-\int_{s_2^-}^{s_2^*}\int_{h_2^-(s_2)}^{h_2^+(x_2)} \{[x_2+\beta(s_2)]\boldsymbol{a}_2(s_2)\cdot\boldsymbol{\gamma}\big(\boldsymbol{r}_2{}^\circ(s_2)+x_2\boldsymbol{b}_2^\circ(s_2),\boldsymbol{r}_2(s_2)+x_2\boldsymbol{b}_2(s_1)\big)(\nu_2^\circ-x_2\mu_2^\circ)\}\,dx_2\,ds_2$$

by virtue of (3.17)–(3.37). This is exactly $\int_{s_2^-}^{s_2^*}[l_2(s_2)-\beta(s_2)\boldsymbol{a}_2(s_2)\cdot\boldsymbol{f}_2(s_2)]\,ds_2$. The arbitrariness of s_1^* then implies that

(3.42) $$l_1(\delta(s_2)) = l_2(s_2)-\beta(s_2)\boldsymbol{a}_2(s_2)\cdot\boldsymbol{f}_2(s_2)\equiv l_2(s_2)+\boldsymbol{k}\cdot[\beta(s_2)\boldsymbol{b}_2(s_2)\times\boldsymbol{f}_2(s_2)].$$

A simplified version of this computation shows that

(3.43) $$\boldsymbol{f}_1(\delta(s_2))=\boldsymbol{f}_2(s_2).$$

Since the stress $\boldsymbol{T}$ depends on just the reference position $\boldsymbol{p}^\circ(s,x)$, definitions (2.16) and (2.17) likewise imply that

(3.44) $$\boldsymbol{n}_1(\delta(s_2))=\boldsymbol{n}_2(s_2),$$

(3.45) $$M_1(\delta(s_2))=M_2(s_2)-\beta(s_2)N_2(s_2)\equiv M_2(s_2)+\boldsymbol{k}\cdot[\beta(s_2)\boldsymbol{b}_2(s_2)\times\boldsymbol{n}_2(s_2)].$$

A straightforward computation using these identities shows that $(\boldsymbol{n}_1,M_1,\boldsymbol{f}_1,l_1)$ satisfy the equilibrium equations (2.20) and (2.21) if and only if $(\boldsymbol{n}_2,M_2,\boldsymbol{f}_2,l_2)$ does.

From (2.25) and (3.29)–(3.31) we find that the constitutive functions transform according to

(3.46)
$$\begin{aligned}
\hat{N}_1(\nu_1,\eta_1,\mu_1,s_1)&=\hat{N}_2([\nu_1-\beta\mu_1]\delta',\eta_1\delta'+\beta',\mu_1\delta',\delta^{-1}(s_1)),\\
\hat{H}_1(\nu_1,\eta_1,\mu_1,s_1)&=\hat{H}_2([\nu_1-\beta\mu_1]\delta',\eta_1\delta'+\beta',\mu_1\delta',\delta^{-1}(s_1)),\\
\hat{M}_1(\nu_1,\eta_1,\mu_1,s_1)&=\hat{M}_2([\nu_1-\beta\mu_1]\delta',\eta_1\delta'+\beta',\mu_1\delta',\delta^{-1}(s_1))\\
&\quad-\beta\hat{N}_2([\nu_1-\beta\mu_1]\delta',\eta_1\delta'+\beta',\mu_1\delta',\delta^{-1}(s_1))
\end{aligned}$$

where the arguments of β, δ, and their derivatives are $\delta^{-1}(s_1)$. By (3.35)–(3.37), (3.44), (3.45) we analogously find transformation formulas for the constitutive functions $\hat{\nu}$, $\hat{\eta}$, $\hat{\mu}$.

4 Curvature

For contact problems, the actual shape of the boundary of the body in contact with the obstacle is of great importance. This shape is determined by the curvature and the elongation of the boundary curve. (These quantities depend on the strains and their derivatives.) We represent the curvature of $\boldsymbol{r}$ in terms of the strains and then formulate a constitutive restriction involving this curvature.

Let ϕ denote the counter-clockwise angle from $\boldsymbol{i}$ to $\boldsymbol{r}'$, so that

(4.1) $$\boldsymbol{r}'=|\boldsymbol{r}'|(\cos\phi\,\boldsymbol{i}+\sin\phi\,\boldsymbol{j}).$$

Then the curvature of $\boldsymbol{r}$ is

(4.2) $$\kappa:=\frac{\phi'}{|\boldsymbol{r}'|}=\frac{\boldsymbol{k}\cdot(\boldsymbol{r}'\times\boldsymbol{r}'')}{|\boldsymbol{r}'|^3}=\frac{\mu(\nu^2+\eta^2)+\nu\eta'-\eta\nu'}{|\boldsymbol{r}'|^3}.$$

We replace ν,η,μ with their constitutive functions (2.32) to obtain

(4.3) $$|\boldsymbol{r}'|^3\kappa=\hat{\mu}(\hat{\nu}^2+\hat{\eta}^2)+\hat{\nu}(\hat{\eta}_N N'+\hat{\eta}_H H'+\hat{\eta}_M M'+\hat{\eta}_s)-\hat{\eta}(\hat{\nu}_N N'+\hat{\nu}_H H'+\hat{\nu}_M M'+\hat{\nu}_s),$$

and then use (2.23) to express N', H', M' in terms of N, H, M and the strains, so that

$$|\boldsymbol{r}'|^3\kappa = |\boldsymbol{r}'|^3\hat{\chi}(N,H,M,s) - (\hat{\nu}\hat{\eta}_N - \hat{\eta}\hat{\nu}_N)\boldsymbol{f}\cdot\boldsymbol{a} - (\hat{\nu}\hat{\eta}_H - \hat{\eta}\hat{\nu}_H)\boldsymbol{f}\cdot\boldsymbol{b} - (\hat{\nu}\hat{\eta}_M - \hat{\eta}\hat{\nu}_M)l \tag{4.4}$$

where

$$|\boldsymbol{r}'|^3\hat{\chi} := \hat{\mu}(\hat{\nu}^2+\hat{\eta}^2) + \hat{\mu}[(\hat{\nu}\hat{\eta}_N - \hat{\eta}\hat{\nu}_N)H - (\hat{\nu}\hat{\eta}_H - \hat{\eta}\hat{\nu}_H)N] - (\hat{\nu}\hat{\eta}_M - \hat{\eta}\hat{\nu}_M)(\hat{\nu}H - \hat{\eta}N) + \hat{\nu}\hat{\eta}_s - \hat{\eta}\hat{\nu}_s \tag{4.5}$$

or, equivalently,

$$\hat{\chi}(N,H,M,s) := (\hat{\nu}^2+\hat{\eta}^2)^{-1/2}[\hat{\mu}(1+\hat{\zeta}_N H - \hat{\zeta}_H N) - \hat{\zeta}_M(\hat{\nu}H - \hat{\eta}N) + \hat{\zeta}_s] \tag{4.6}$$

where $\zeta := \arctan(\eta/\nu) \equiv \phi - \theta$ is the shear angle, $\hat{\zeta} := \arctan(\hat{\eta}/\hat{\nu})$ is the corresponding constitutive function, and the arguments of the constitutive functions are N, H, M, s. (Alternatively, we could express the curvature as a function of the strains by substituting the constitutive equations (2.25) into (2.23), using Cramer's Rule (justified by (2.27)) to solve for ν' and η', and substituting these representations into (4.2).)

We shall find it convenient to consider materials for which the curvature in the actual configuration minus that for the reference configuration has the same sign as M under "natural" conditions, i.e., when there is no body force or body couple: $\boldsymbol{f} = \boldsymbol{0}$, $l = 0$. We say that a rod theory for a body $\mathcal{B}$ of (2.2) has *normal bending with respect to a skeleton* $\{\boldsymbol{r}^\circ, \boldsymbol{b}^\circ\}$ if it satisfies the constitutive restriction

$$[\hat{\chi}(N,H,M,s) - \kappa^\circ]M > 0 \quad \text{for} \quad M \neq 0. \tag{4.7}$$

(If the base curve $\boldsymbol{r}^\circ$ of a rod in the reference configuration is a straight line of centroids with $\eta^\circ = 0$ and if $\hat{\zeta}$ does not depend explicitly on s, then (2.29) implies that $\hat{\chi}$ is odd in M; condition (4.7) strengthens this special case by ensuring that the curvature function $\hat{\chi}$ vanishes only at $M = 0$.) The condition (4.7), made complicated by the shearability as (4.3) shows, prevents the paradoxical bending behavior described by [10].

One could consider the restriction that (4.7) hold for every skeleton (the explicit formulation of which could be effected by a complicated version of the process by which (2.8) is derived from (2.7)). But there is no need to study this restriction because there are bodies $\mathcal{B}$ for which (4.7) can hold merely for one special skeleton and not for any others: Choose two skeletons which give equivalent theories with $\kappa^\circ = 0, \eta^\circ = 0, \hat{\zeta}_s = 0$ and assume that in each case (4.7) holds for all N, H, M ($M \neq 0$). By the symmetry (2.28),

$$\hat{\chi}(N,0,M)M = \frac{\hat{\mu}(N,0,M)M}{\hat{\nu}(N,0,M)}\left(1 - \frac{\hat{\eta}_H(N,0,M)}{\hat{\nu}(N,0,M)}N\right) \tag{4.8}$$

for each skeleton. There is an $\varepsilon > 0$ such that for each skeleton,

$$1 - \frac{\hat{\eta}_H(N,0,M)}{\hat{\nu}(N,0,M)}N > 0 \tag{4.9}$$

for all $|M| \leq 1$, $|N| \leq \varepsilon$. By (4.7)–(4.9), $\hat{\mu}(N,0,M)M > 0$ for all M, N with $0 < |M| \leq 1$, $|N| \leq \varepsilon$. Thus $\hat{\mu}_2 > 0$ if $0 < M_2 < 1$, $|N_2| < \varepsilon$. Using $\mu_1 = \mu_2/\delta'$, $\delta' > 0$, $M_1 = M_2 - \beta N_2$, we get $\hat{\mu}_2(N_2, 0, M_2)(M_2 - \beta N_2) > 0$, so that $M_2 > \beta N_2$ for all M_2, N_2 with $0 < M_2 < 1$, $|N_2| < \varepsilon$, which is a contradiction. On the other hand, if we have a skeleton enjoying the symmetry (2.29) (e.g., if $\boldsymbol{r}^\circ$ is a straight curve of centroids), then (4.8) holds for $|M| < 1$, $|N| < \varepsilon$ (for some small $\varepsilon > 0$). By the same argument as above we conclude that no other skeleton can satisfy (4.7). Thus, in general, it cannot be expected that (4.7) holds for more than one skeleton. On the other hand, if there is a straight curve of centroids and (4.7) holds for some skeleton, then it can only hold for the skeleton based upon the curve of centroids.

5 Applications

In this section we apply the theory developed above to some simple problems that exhibit novel effects. We limit our attention to uniform rectangular beams of scaled length 1, for which (2.2) reduces to

$$\mathcal{B} = \{s\boldsymbol{i} + x\boldsymbol{j} : 0 \leq s \leq 1, -h \leq x \leq h\} \tag{5.1}$$

where $h > 0$ is a constant. We consider only skeletons of the form

$$\boldsymbol{r}^\circ = s\boldsymbol{i} + \beta\boldsymbol{j}, \qquad \boldsymbol{b}^\circ = \boldsymbol{j} \tag{5.2}$$

with $\beta \in [-h, h]$ a constant. (Thus (3.1) holds, $\mu^\circ = 0$, and $\delta(s) = s$.) We assume that the material has normal bending with respect to a given skeleton. In view of the remarks following (4.7), this means that $\boldsymbol{r}^\circ$ for this skeleton must be the line of centroids of the rod, so that $\beta = 0$ and $-h^- = h^+ = h$ (note that $h^\pm$ in $(2.2)_2$ depend on β). We accordingly denote variables associated with this skeleton by the index c (for centroid). Variables associated with typical skeletons bear no indices.

Example 1. We consider the deformation of a rod whose left end $s = 0$ is welded to a "vertical" wall (parallel to $\boldsymbol{j}$) and that is subjected to a prescribed concentrated "downward" force $-\lambda\boldsymbol{j}$, with λ positive, applied at the point $\boldsymbol{r}(1)$ (cf. Figure 2a). There are no other externally applied forces. We first study the curvature of $\boldsymbol{r}$ while the load acts at $\boldsymbol{r}_c(1)$ and then we study the effect of applying the load at $\boldsymbol{r}(1)$ on the curvature of $\boldsymbol{r}_c$. For this problem, varying the base curve is equivalent to varying the point on the section $s = 1$ at which the force $-\lambda\boldsymbol{j}$ is applied.

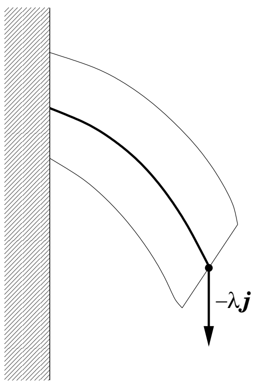

Figure 2a. Deformation of a rod subject to a terminal force applied at the midpoint of the end. The material curves parallel to the curve of centroids and lying above it are concave, while such curves lying below it are convex near the right end.

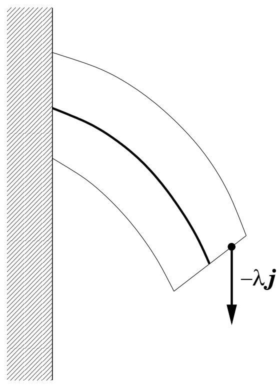

Figure 2b. If a terminal force is applied above the midpoint of the end, then the deformed curve of centroids is concave near the right end.

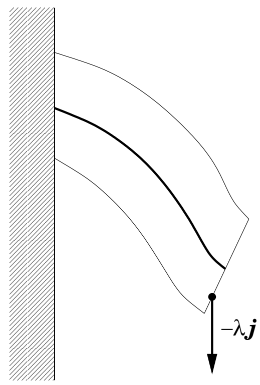

Figure 2c. If a terminal force is applied below the midpoint of the end, then the deformed curve of centroids is convex near the right end.

The boundary conditions are

$$\boldsymbol{r}(0) = \boldsymbol{0}, \quad \theta(0) = 0, \quad \boldsymbol{n}(1) = -\lambda\boldsymbol{j}, \quad M(1) = 0. \tag{5.3}$$

The equilibrium equation (2.20) implies that

$$\boldsymbol{n}(s) = -\lambda\boldsymbol{j}, \tag{5.4}$$

which implies that

$$N(s) = -\lambda \sin\theta(s), \quad H(s) = -\lambda\cos\theta(s), \tag{5.5}$$

Thus

$$\nu(s) = \hat{\nu}(-\lambda\sin\theta(s), -\lambda\cos\theta(s), M(s)), \quad \eta(s) = \hat{\eta}(-\lambda\sin\theta(s), -\lambda\cos\theta(s), M(s)). \tag{5.6}$$

Thus the substitution of (5.6) into $(2.23)_3$ and the use of (2.32) produces the system of two first-order equations:

$$\begin{aligned} M'(s) &= \lambda\cos\theta(s)\hat{\nu}(-\lambda\sin\theta(s), -\lambda\cos\theta(s), M(s)) \\ &\quad - \lambda\sin\theta(s)\hat{\eta}(-\lambda\sin\theta(s), -\lambda\cos\theta(s), M(s)) \\ \theta'(s) &= \hat{\mu}(-\lambda\sin\theta(s), -\lambda\cos\theta(s), M(s)) \end{aligned} \tag{5.7}$$

subject to the boundary conditions $\theta(0) = 0$, $M(1) = 0$.

Standard regularity arguments show that the strains ν, η, μ are continuous. In general, this problem admits multiple solutions with loops when λ is large enough. (In view of our scaling, λ can be made large either by increasing the magnitude of the terminal force or by increasing the actual length of the rod.) We limit our attention to solutions for which

$$\boldsymbol{r}'(s)\cdot\boldsymbol{i} \equiv \nu(s)\cos\theta(s) - \eta(s)\sin\theta(s) > 0 \quad \text{for} \quad 0 \le s \le 1. \tag{5.8}$$

When $\lambda = 0$, it follows from (5.6) and the properties of $\hat{\eta}$ that $\eta = 0$ and it follows from (5.7) that $\theta = 0 = M$. Continuation theory [1, Chap. 3] can be used to show that emanating from the trivial solution pair $((\theta, M), \lambda) = ((0,0), 0)$ is a branch of nontrivial solution pairs $((\theta, M), \lambda)$ of (5.7). Consequently (5.8) holds for sufficiently small λ. (Actually much more can be proved by applying a phase-plane analysis to the problem; cf. [1, Chap. 5].)

It follows from (2.21) and (5.8) that

$$M'(s) = \lambda\boldsymbol{r}'(s)\cdot\boldsymbol{i} > 0, \tag{5.9}$$

so that$(5.3)_4$ yields

$$M(s) < 0 \quad \text{for} \quad 0 \le s < 1. \tag{5.10}$$

Now we consider the case in which the load is applied at the end of the curve of centroids, i.e., at $\boldsymbol{r}_{\rm c}(1)$. Under the assumption that (4.7) applies to the skeleton c, we immediately obtain from (5.10) that

$$\kappa_{\rm c}(s) < 0 \quad \text{for} \quad 0 \le s < 1, \quad \kappa_{\rm c}(1) = 0. \tag{5.11}$$

Now we introduce a second skeleton of the form (5.2) with $\beta \in [-h, h]$, $\beta \neq 0$. Thus (3.35), (3.36), (3.37) yield

$$\mu = \mu_{\rm c}, \quad \nu = \nu_{\rm c} - \beta\mu_{\rm c}, \quad \eta = \eta_{\rm c}. \tag{5.12}$$

It follows from (4.2) that

$$\operatorname{sign}\kappa = \operatorname{sign}\{\mu_{\rm c}[(\nu_{\rm c} - \beta\mu_{\rm c})^2 + {\eta_{\rm c}}^2] + (\nu_{\rm c} - \beta\mu_{\rm c})\eta_{\rm c}' - \eta_{\rm c}(\nu_{\rm c}' - \beta\mu_{\rm c}')\}. \tag{5.13}$$

Since $\kappa_{\rm c}(1) = 0$, it then follows from (4.2) that

$$\operatorname{sign}\kappa(1) = -\operatorname{sign}\{\beta[{\mu_{\rm c}}^2(2\nu_{\rm c} - \beta\mu_{\rm c}) + \mu_{\rm c}\eta_{\rm c}' - \eta_{\rm c}\mu_{\rm c}'](1)\}. \tag{5.14}$$

Since $\boldsymbol{r}_{\rm c}^{\circ}$ is a straight curve of centroids, (2.29) implies that $\mu_{\rm c}(1) = 0$ because $M_{\rm c}(1) = 0$. Hence $\operatorname{sign}\kappa(1)$ $= \operatorname{sign}\beta\eta_{\rm c}(1)\mu_{\rm c}'(1)$. To show that this is not zero, we differentiate $\mu_{\rm c}(s) = \hat{\mu}_{\rm c}(N_{\rm c}(s), H_{\rm c}(s), M_{\rm c}(s))$ with respect to s and use (5.5), (5.9), $\mu_c(1) = 0$, $\partial\hat{\mu}_c/\partial M > 0$ to get $\mu_c'(1) > 0$. From (5.8) and (5.3) we get $\theta_c(s) \in (-\pi/2, \pi/2)$ and, thus, $H_c(s) < 0$, $\eta_c(s) < 0$. Consequently $\operatorname{sign}\kappa(1) = -\operatorname{sign}\beta$. Thus, if the load is applied at the end point $\boldsymbol{r}_c(1)$ of the curve of centroids, then a "parallel" base curve in the upper part of the rod is concave near $s = 1$ and a "parallel" base curve in the lower part of the rod is convex near $s = 1$, while $\kappa_c(1) = 0$ (see Figure 2a).

Now, we content ourselves with a complementary result. We take a skeleton of the form (5.2) with $\boldsymbol{r}^\circ = \boldsymbol{r}_c^\circ + \beta\boldsymbol{b}_c^\circ$, $\boldsymbol{b}^\circ = \boldsymbol{b}_c^\circ$, $0 \neq \beta \in [-h, h]$ and take the force $-\lambda\boldsymbol{j}$ to be applied at $\boldsymbol{r}(1)$, i.e., we take $\boldsymbol{r}$ to be the image of the base curve. In contrast to the previous situation, we now study $\operatorname{sign}\kappa_c(1)$. From (3.46) we obtain

$$M = M_c + \beta N_c, \qquad N = N_c. \tag{5.15}$$

Since $N(0) = 0$ by (5.5), it follows from (5.10),(5.15), (4.7) that $\kappa_c(0) < 0$. Since κ_c is continuous by standard regularity arguments, it follows that κ_c is negative near $s = 0$, so the image of the centroid is concave here.

Below we show that

$$N(s) \equiv N_c(s) > 0 \quad \text{for} \quad 0 < s \leq 1. \tag{5.16}$$

Equations (5.15) and $(5.3)_4$ imply that

$$M_c(1) = -\beta N_c(1). \tag{5.17}$$

If $\beta > 0$ (e.g., if the top of the body were taken to be the base curve), then (5.17), (5.16), and (4.7) would imply that $\kappa_c(1) < 0$, so that the image of the line of centroids would be concave near $s = 1$ (see Figure 2b). On the other hand, if $\beta < 0$, we likewise find the more surprising result that $\kappa_c(1) > 0$, so that the image of the line of centroids would be convex near $s = 1$ (see Figure 2c).

We now verify (5.16): Since $\theta(0) = 0$ by (5.3) and since $M_c(0) = M(0) < 0$ by (5.10) and (5.15) because $N(0) = 0$, it follows from (2.29) that $\mu_c(0) < 0$ and from (5.12) that $\mu(0) < 0$. Thus $\theta(s) < 0$ and $N(s) > 0$ for small positive s. Suppose that there were a first value σ of s in $[0, 1]$ at which N were to vanish. By the continuity of θ, either $\theta(\sigma) = 0$ or $\theta(\sigma) = -\pi$. But the latter possibility violates (2.7) and (5.8). We therefore consider just the former case. Since $\theta(s) < 0$ for $0 < s < \sigma$, it follows that $\mu(\sigma) \geq 0$. Then (2.29) implies that $M(\sigma) \geq 0$, in violation of (5.10) provided that $\sigma < 1$ or $M(1) < 0$. Suppose that $\sigma = 1$ and $M(1) = 0$ and, thus, also $\theta(1) = 0$, $N(1) = 0$, $M_c(1) = 0$ by (5.15), $\mu_c(1) = \mu(1) = 0$ by (2.29) and (5.12). Differentiating $(5.7)_2$ we get $\theta''(1) > 0$ by (5.9), (2.27). But this inequality is incompatible with $\theta(s) < 0$ on $(0, 1)$ and $\theta'(1) = 0$. This contradiction yields (5.16).

Thus there is a significant qualitative difference in the curvature of the line of centroids for $\beta > 0$ and $\beta < 0$. This difference does not appear for the corresponding problems for unshearable rods. Numerical simulations of analogous 2-dimensional problems of linear elasticity, exhibited in Figure 3, show the same curvature effects.

Figures 3a,b,c, respectively correspond to those of Figures 2a,b,c. Note the singular behavior at the corners and at the places where the concentrated loads are applied.

The simulations shown here were done with an adaptive finite-element code with about 16,000 nodes (so that the computational grid used is much finer than that seen in the figures). The body $\mathcal{B}$ for these simulations has $h^+ = -h^- = \frac{1}{4}$. (We use very thick rods for these 2-dimensional computations because the effects of curvature are quite pronounced.) The position of the left edge $s = 0$ is fixed. The concentrated load is approximated by a surface traction distributed along two of the squares in the figure at the right edge. The simulations for this and all our other examples are done for rubber with $\lambda = 0.4 \times 10^5$ kg/cm^2, $\mu = 0.012 \times 10^5$ kg/cm^2 [3, Sec. 3.8]. The grids in all figures show deformed squares.

Example 2. We adopt the same geometry as in Example 1, but replace the terminal load by the weight of the rod. If the density of the rod is constant and if we take $\boldsymbol{r}^\circ$ to be the line of centroids, then (2.18) and (2.19) imply that $\boldsymbol{f}$ and l have the forms

$$\boldsymbol{f}(s) = -\omega\boldsymbol{j}, \qquad l = 0, \tag{5.18}$$

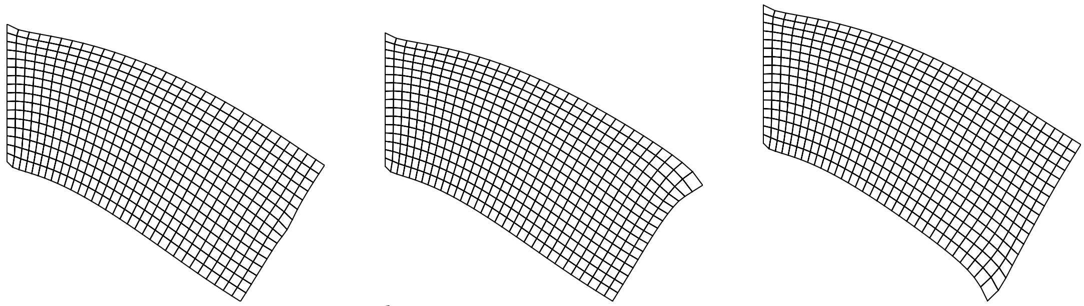

a. b. c.

Figure 3. Numerical simulations of 2-dimensional problems of linear elasticity corresponding to those shown in Figure 2.

where $\omega > 0$ is the constant weight per unit of s. The boundary conditions are

$$\boldsymbol{r}(0) = \boldsymbol{0}, \quad \theta(0) = 0, \quad \boldsymbol{n}(1) = 0, \quad M(1) = 0. \tag{5.19}$$

Then (2.20) implies that $\boldsymbol{n}(s) = -\omega(1-s)\boldsymbol{j}$, whence (2.22) yields

$$N(s) = -\omega(1-s)\sin\theta, \qquad H(s) = -\omega(1-s)\cos\theta. \tag{5.20}$$

As in the Example 1 we are justified in adopting (5.8). Then it and $(2.23)_3$ yield

$$M'(s) = \omega(1-s)\boldsymbol{r}'(s)\cdot\boldsymbol{i}, \qquad M(s) < 0 \quad \text{for} \quad 0 \le s < 1. \tag{5.21}$$

It follows from(2.29) that

$$\mu(s) < 0 \quad \text{for} \quad 0 \le s < 1, \qquad \mu(1) = 0. \tag{5.22}$$

We cannot deduce from (4.7) the analogous result that κ is negative because $\hat{\chi}$ is not the curvature for this problem. To determine the curvature, we use (4.3). The first term on the right-hand side of (4.3) is clearly negative for $s < 1$. Using (5.19), the symmetry conditions (2.28) and (2.29), the fact that the reference configuration is stress-free, and (5.20), we find that the last two summands of (4.3) at $s = 1$ reduce to

$$\omega\hat{\eta}_H(0,0,0)\cos\theta(1) > 0, \tag{5.23}$$

the inequality following from (2.27). Thus the deformed centroid is convex near $s = 1$. This result is entirely due to the shearability of the rod.

To determine the curvature at $s = 0$, we could again resort to the formula (4.3), but now the last two terms are complicated with no obvious sign, suggesting that the curvature depends on constitutive properties. Equation (4.4) yields

$$|\boldsymbol{r}'|^3\kappa = |\boldsymbol{r}'|^3\hat{\chi} + \omega[(\hat{\nu}\hat{\eta}_N - \hat{\eta}\hat{\nu}_N)\sin\theta + (\hat{\nu}\hat{\eta}_H - \hat{\eta}\hat{\nu}_H)\cos\theta]. \tag{5.24}$$

Since $\theta(0) = 0$ by (5.19), it follows from (5.20) that $N(0) = 0$ and $H(0) = -\omega$, so that (4.5) and (5.24) yield

$$|\boldsymbol{r}'|^3\kappa = \hat{\mu}(\hat{\nu}^2 + \hat{\eta}^2) - \omega\hat{\mu}(\hat{\nu}\hat{\eta}_N - \hat{\eta}\hat{\nu}_N) + \omega\hat{\nu}(\hat{\nu}\hat{\eta}_M - \hat{\eta}\nu_M) + \omega(\hat{\nu}\hat{\eta}_H - \hat{\eta}\hat{\nu}_H) \quad \text{at} \quad s = 0, \tag{5.25}$$

with the arguments $(0, -\omega, M(0))$ in the constitutive functions. We know that $\mu(0) < 0$ and $\eta(0) < 0$, but this information is insufficient to give a sign to (5.25), even in the case that the constitutive equations were uncoupled, so that $\hat{\nu}_H = 0 = \hat{\eta}_N$ (an extreme version of (2.28)). The sign depends on the constitutive response, especially the strength of the rod in resisting flexure and shear (which in turn depends on the thickness), and on the size of ω, which depends on the actual length. We leave as an exercise for the interested reader the computation, analogous to that for Example 1, of how the curvature depends on the choice of the base curve. A 2-dimensional simulation of this problem under conditions like those of Figure 3 is given in Figure 4a.

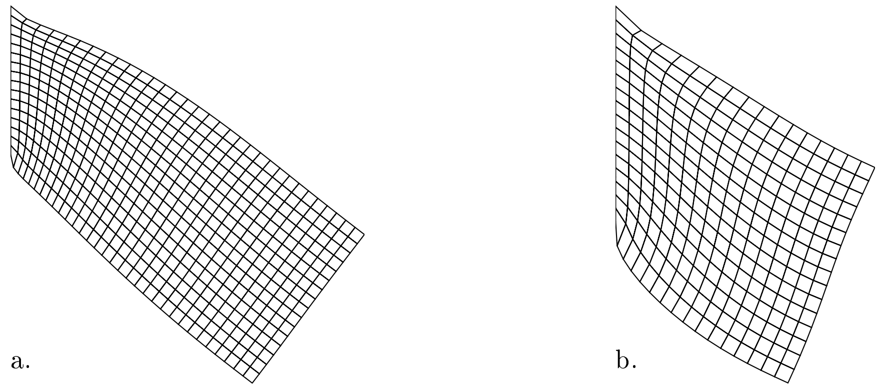

Figure 4. Numerical simulations of 2-dimensional problems of linear elasticity for the deformation of rectangular bodies under their own weight when their left edges are welded to a vertical wall.

If we take the body to have a shape that is the antithesis of a rod-like shape, i.e., if the thickness is of the same order as the length, then a 2-dimensional simulation of the equilibrium state for this body under its own weight gives Figure 4b. Note that the deformed images of the material lines parallel to the line of centroids are each convex. It is amusing to note that the formal treatment of such a problem within our rod theory gives the same convexity (even though the rod theory is patently inappropriate for the treatment of such a problem): Suppose that $s^- = 0$ and that the length s^+ is small. Then by exploiting (5.20)–(5.21), we could show that N, H, M are small, whence it follows that the deformed configuration is close to the reference configuration: $\nu \approx 1$, $\eta, \mu \approx 0$. In this case, $\hat{\eta}_M \ll \hat{\eta}_H$, so that (5.24) is dominated by $\omega\nu\hat{\eta}_H > 0$, i.e., a very short rod is convex.

Example 3. We study problems in which the material points of the base curve lying in an interval of the form $[0, \sigma]$ with $\sigma < 1$ are in contact with a rigid horizontal obstacle, and the rest of the base curve lies above the obstacle. In particular, we assume that there is a hinge at $\boldsymbol{r}(1)$ that is fixed at a point lying above the obstacle and we assume that there is a couple $M(1)$ applied to the rod about the hinge that is a sufficiently large positive number. See Figure 5a. The most natural choice for the base curve is the bottom of the rod, as shown in Figure 5a. Contact problems for different choices of base curves can be realized by rods with longitudinal flanges that lie on horizontal obstacles, as shown in Figures 5b,c. We assume that the only loads on the rod are the prescribed couple $M(1)$ about $\boldsymbol{r}(1)$, the reaction at $\boldsymbol{r}(1)$, and the reaction to contact with the obstacle.

There are several open questions for contact problems for rods, which we finesse by making suitable assumptions: For example, given the conditions at $\boldsymbol{r}(1)$, can one prove that there is a solution of the equilibrium equations with the contact region an interval of the form we have taken? If there is such a solution, is it the only one?

On the interval $[0, \sigma]$ of contact,

$$\boldsymbol{r}' \cdot \boldsymbol{j} \equiv \nu \sin\theta + \eta \cos\theta = 0, \quad \kappa = 0 \quad \text{for} \quad s \in [0, \sigma]. \tag{5.26}$$

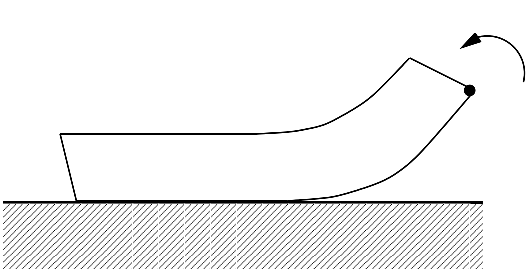

Figure 5a. The left part of a rod is pressed against a rigid horizontal obstacle by a couple applied at the right end of the rod.

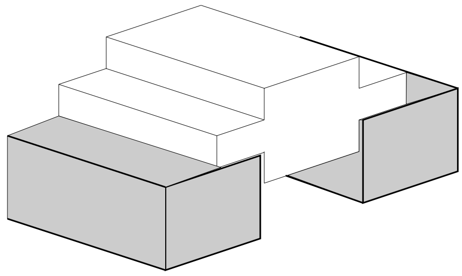

Figure 5b. For a body with flanges the contact curve need not be a bottom (or top) curve of the corresponding 2-dimensional body $\mathcal{B}$ (cf. (2.2)).

We assume that the contact is frictionless, so that $\boldsymbol{f}(s) = f(s)\boldsymbol{j}$ with $f(s) = 0$ for $\sigma < s < 1$. Since the contact force acts only on the base curve, it induces no couple l by (2.19). For shearable rods undergoing this kind of contact, Schuricht [8] proved that f is continuous on $(0, \sigma]$, that $f(s) \geq 0$ for $0 \leq s \leq \sigma$, that $f(s) = 0$ on $(\sigma, 1)$ where there is no contact, that there can be a jump in f at $s = \sigma$ (which we will exploit), and that the stress resultants N, H, M and the strains ν, η, μ are continuous on $(0, 1)$.

In view of these results, the difference in the limits of (4.4) as s approaches σ from above and below is

$$|\boldsymbol{r}'(\sigma)|^3 \kappa(\sigma+) = f(\sigma-)[(\hat{\nu}\hat{\eta}_N - \hat{\eta}\hat{\nu}_N)\sin\theta + (\hat{\nu}\hat{\eta}_H - \hat{\eta}\hat{\nu}_H)\cos\theta]|_{s=\sigma}. \tag{5.27}$$

Since (2.8) implies that $\cos\theta(\sigma)$ cannot vanish on $[0, \sigma]$, we can solve (5.26) for η and substitute the result into the right-hand side (5.27), which becomes

$$f(\sigma-)\frac{\hat{\nu}}{\cos\theta}[\hat{\nu}_N \sin^2\theta + (\hat{\nu}_H + \hat{\eta}_N)\cos\theta\sin\theta + \hat{\eta}_H \cos^2\theta]|_{s=\sigma}; \tag{5.28}$$

the expression in brackets is a positive-definite quadratic form in $\hat{\nu}_N, \hat{\nu}_H, \hat{\eta}_N, \hat{\eta}_H$ by virtue of (2.27). Thus (5.27) says that the jump in curvature has the same sign as the non-negative $f(\sigma-)$, which is not surprising.

To determine whether $f(\sigma-)$ is positive, we study (4.4) at $\sigma-$, which says that $f(\sigma-)$ has the same sign as $\hat{\chi}$ at σ by virtue of the positivity of the quadratic form in (5.28). (Note that $s \mapsto \hat{\chi}(N(s), H(s), M(s))$ is continuous.) We wish to adopt (4.7), so that $f(\sigma-)$ would have the same sign as $M(\sigma)$, which we now study. In view of the remarks following (4.7), however, we can only use (4.7) when the base curve is the line of centroids. We limit our analysis to this case (cf. Figure 5c.) In accord with the version of Figure 5a appropriate for the base curve as the line of centroids, we assume that $M(0) = 0$. There is, however, a concentrated force at the left end. In particular, (2.20), (2.21), and the results in [9, Example 2] imply that there is an $f_0 > 0$ such that

$$\boldsymbol{n}(s) = -\left(f_0 + \int_0^s f(t)\,dt\right)\boldsymbol{j}, \tag{5.29}$$

$$M(\sigma) = \int_0^\sigma \left[\boldsymbol{r}'(s)\cdot\boldsymbol{i}\left(f_0 + \int_0^s f(t)\,dt\right)\right] ds. \tag{5.30}$$

Since $\boldsymbol{r}'(s) \cdot \boldsymbol{i} > 0$ a.e. on $[0, \sigma]$ by (2.8), since $f_0 > 0$, and since $f \geq 0$ everywhere, it follows that $M(\sigma) > 0$. Thus $f(\sigma-) > 0$, whence $\kappa(\sigma+) > 0$. This means that the rod lifts off the obstacle at σ, and the solution has the expected form. Unfortunately, we found no attractive constitutive replacement for (4.7) that would give comparable intuitively obvious conclusions for base curves other than the line of centroids.

6 Comments

In many problems for rod (and shell) theories, the constitutive equations based on a special choice of base curve (or surface) enjoy a variety of symmetries. If constitutive equations with respect to another base curve are used, say, to handle contact problems, then these symmetries are hidden. It is only by exploiting results on the change of base curve that we can have access to the hidden symmetries. This difficulty unavoidably arises in another context: There are special choices of base curves (and surfaces) that considerably simplify the inertia terms in the equations of motion for rods (and shells). Unfortunately, when a rod (or shell) is curved, this choice of base curve (or midsurface) does not give a concomitant simplification to the constitutive equations, and in particular, may result in the hiding of constitutive symmetries taken with respect to a centroidal base curve (or midsurface).

This work shows that the theory of constitutive equations needed for concrete problems is necessarily much richer than that needed to ensure the existence of solutions. We used the change of base curve to develop new kinds of constitutive restrictions, distinct from those associated with monotonicity and coercivity, and we showed that these new restrictions led to new qualitative effects. Our higher-dimensional computations suggest that these new effects capture those that might be expected in 2-dimensional theories.

It is clear that the methods of this paper are valid for much more intricate rod and shell theories.

Acknowledgment. We are greatly indebted to U. Weikard of the Universität Duisburg for the two-dimensional numerical computations. Some of the research reported here was performed by both authors at the Max Planck Institute for Mathematics in the Sciences, Leipzig. The work of Antman reported here was supported in part by ARO-MURI97 Grant No. DAAG55-97-1-0114 to the Center for Dynamics and Control of Smart Structures and by NSF Grant DMS 99 71823.

References

[1] S.S. Antman, *Nonlinear Problems of Elasticity*, Springer, 1995.

[2] S.S. Antman and F. Schuricht, Incompressibility in Rod and Shell Theories, *Math. Modelling Num. Anal.* **33** (1999), 289–304.

[3] P. G. Ciarlet, *Mathematical Elasticity, Vol. I: Three-Dimensional Elasticity*, North Holland, 1988.

[4] E. and F. Cosserat, *Théorie des corps déformables*, Hermann, 1909.

[5] L. Euler, *Additamentum I de curvis elasticis, methodus inveniendi lineas curvas maximi minimivi proprietate gaudentes*, Bousquent, Lausanne, 1744, in *Opera Omnia* I, Vol. 24, 231–297.

[6] G. Kirchhoff, Über das Gleichgewicht und die Bewegung eines unendlich dünnen elastischen Stabes, *J. reine angew. Math.* **56** (1859) 285–313, in *Gesammelte Abhandlungen*, 285–316.

[7] F. Schuricht. A variational approach to obstacle problems for shearable nonlinearly elastic rods, *Arch. Rational Mech. Anal.* **140** (1997) 103–159.

[8] F. Schuricht. Regularity for shearable nonlinearly elastic rods in obstacle problems, *Arch. Rational Mech. Anal.* **145** (1998) 23–49.

[9] F. Schuricht, Straight configurations of shearable nonlinearly elastic rods, *SIAM J. Appl. Math.* **60** (2000) 1017–1036.

[10] F. Schuricht and B. Werner, Paradoxical bending behavior of shearable nonlinearly elastic rods, *J. Elasticity* **50** (1998) 27–48

[11] S. P. Timoshenko, On the correction for shear of the differential equations for transverse vibrations of prismatic bars, *Phil. Mag.*, Ser. 6, **41** (1921) 744–746.